IEEE INSTRUMENTATION & MEASUREMENT SOCIETY

Received 22 June 2023; accepted 9 July 2023. Date of publication 1 August 2023; date of current version 22 August 2023.
The review of this article was arranged by Associate Editor Nan Li.

Digital Object Identifier 10.1109/OJIM.2023.3300436

Residence Time Difference Fluxgate Magnetometer in "Horseshoe-Coupled" Configuration

CLAUDIA FERRO [1] (Graduate Student Member, IEEE), BRUNO ANDÒ [1] (Senior Member, IEEE), CARLO TRIGONA [1] (Member, IEEE), ADI R. BULSARA [2], AND SALVATORE BAGLIO [1] (Fellow, IEEE)

[1]Dipartimento di Ingegneria Elettrica Elettronica e Informatica, University of Catania, 95124 Catania, Italy

[2]Naval Information Warfare Command, San Diego, CA 92152, USA

CORRESPONDING AUTHOR: C. FERRO (e-mail: claudia.ferro@phd.unict.it)

This work was supported in part by the Sicilian Region under Project POR 1.1.5 "IRMA"; in part by the "IRMA Parkinson Cyclone in Life" Project under Grant 088690110504 and Grant CUP G69J18001070007 (Azione 1.1.5 del POR FESR 2014–2020); and in part by the 4 FRAILTY—"Sensoristica intelligente, infrastrutture e modelli gestionali per la sicurezza di soggetti fragili" Project, area di specializzazione "Tecnologie per gli ambienti di Vita" under Grant ARS01_00345–CUP: E66C18000200005.

ABSTRACT Fluxgate magnetometers are, possibly, the simplest and most convenient magnetic flux sensors and yet capable, in controlled environments and with some well-conceived technical embellishments, to detect magnetic fields in the order of 50 nT or less. In practice, they are limited by the presence of unwanted or contaminating signals, these include the sensor noise floor as well as noise-contamination of the target signal of interest. The residence time difference (RTD) readout technique was conceived as a readout protocol that is remarkable in its simplicity and its ability to outperform the conventional "second harmonic" readout. In this work, we address the issue of the fluxgate sensitivity in the presence of spurious dc magnetic field signals, while ensuring that the sensor delivers a high responsivity to the target signal. This is achieved through a "Horseshoe Configuration": three rod-core fluxgates are connected in series forming a U (horseshoe) and the output is drawn only from one secondary (or pick-up) coil using the RTD readout mechanism. The two branches of this configuration yield a differential mechanism *vis-a-vis* the (unwanted) external magnetic field, while the magnetic target is "localized" by being placed in or in the proximity of the air gap of the horseshoe. A theoretical analysis of the efficacy of this configuration considering the geometry, the demagnetizing effect, and the sensing mechanism is carried out. The results confirm the theoretical assumptions: the sensitivity to the (spurious) external magnetic fields can be reduced and the sensitivity to the target signal enhanced, with a concomitant enhanced tolerance to noise. The results appear promising for the detection of very small magnetic fields, e.g., the magnetic fields encountered in the project "IRMA Parkinson Cyclone in Life" for the noninvasive diagnosis of neuroferritinopathies through the detection of a few milligrams of iron inside the brain.

INDEX TERMS CoFeSiB flexible core, dc magnetic field measurements, Horseshoe-coupled structure, residence time difference (RTD)-fluxgate, tolerance to noise.

I. INTRODUCTION

FLUXGATE magnetometers have been used for several years in a wide variety of different applications [1], [2], [3], [4], [5], [6] involving the detection and quantification of (dc or low-frequency ac) magnetic fields, in the range of 10^{-12} to 10^{-4} Tesla. Recently, the authors have introduced a time domain readout that is "event based" and underpinned by a calculation of the residence time difference (RTD) [7], [8], [9] as an efficient alternative to the traditional second harmonic technique [10], [11], [12]. In the RTD setup, the fluxgate (in its simplest realization) consists of a soft magnetic core wound with primary (or excitation) and secondary (or pick-up) coils.

The RTD fluxgate has been developed [13], [14], [15], [16] with specific applications in mind, in particular biomedical applications [17]. The main challenges in these applications come from the ability of the sensor to suppress environmental and electronic noise while extracting the information buried in weak target signals. To this aim, the literature is replete with efforts to model the environmental contributions to fluxgate noise [18] and then develop noise mitigation schemes to enhance the noise immunity of the sensor in different ways: using different core materials [19], [20], [21], analyzing the effect to use more than one wire for the core [22], developing new harmonic analysis algorithms (with the second harmonic readout) [23], but most of the studies have been conducted over new geometries able to reduce the demagnetization factor and then enhance sensitivity and reduce the noise [24], [25]. In particular, in the last few years, much attention has been devoted to race-track geometries [26], [27] thanks to their lower demagnetization (compared to the ring-core) and the lower noise floor (compared to the rod core) [28]. For the RTD readout, only a study about the optimal geometry of a PCB fluxgate to minimize the demagnetizing effect has been carried out [29].

We note that, in addition to the "single-core" RTD fluxgate, "coupled-core RTD fluxgates" have been introduced together with nonlinear dynamics-based signal analysis strategies, yielding improved signal detection performance compared to the single-core device. A good overview of the single and coupled-core fluxgates is provided in [30]. Despite their enhanced sensitivity, however, coupled-core RTD fluxgates remain quite complex compared to their single-core counterparts whose strength lies in the combination of acceptable performance for a particular application, and the simplicity of its architecture. We note that, for the detection of weak cyclic magnetic field signals, advanced configuration techniques, (one good example is "injection locking" [31]) can yield very good performance (exemplified by noise suppression in the bandwidth of interest), when applied to the coupled-core magnetometer.

In this article, a novel coupling scheme for single core RTD fluxgates is presented with the aim of performing high sensitivity measurements of very weak static magnetic field signals, while retaining enhanced (compared to a conventional single-core device) noise tolerance. The coupling mechanism uses three single core RTD fluxgates physically connected in a horseshoe configuration and electrically connected through the same bias current to obtain a reduction of the undesired disturbance effects while at the same time enhancing the response to the target. We start with the model of the coupled sensor system, together with some insights on the effects of demagnetization and noise in Section II. The proposed horseshoe architecture is presented in Section III and validated through experiments, with the matching of the results to the model shown in Sections IV and V. Finally, applications to the magnetic measurements in the context of neurodegenerative diseases (which result in an anomalous accumulation of iron in the basal ganglia) will be presented in Section V. It should be declared that Sections IV and V include some content from a master's thesis [32] of one of the authors. We conclude with some final remarks on potential future evolutions of this sensor.

II. BACKGROUND: THE RTD PRINCIPLE AND THE ISSUE OF NOISE

In the ferromagnetic core, magnetic field intensity H and the magnetic field induction B are related by a hysteretic characteristic. Therefore, the dynamics may be characterized via the "particle-in-potential" paradigm as a two-state (or bistable) dynamic system. When detection of a weak (usually dc) magnetic field, having amplitude smaller than the energy barrier (roughly equivalent to the coercivity) separating the two stable states is desired, one needs to cause the device to switch between its stable states. This is accomplished by the fluxgate mechanism: a periodic current flowing through the excitation coil produces a magnetic field in the core, which periodically saturates (corresponding to switching between the stable steady states on a time-scale controlled by the signal frequency). This so-called "excitation signal" is, typically, a sinusoid or triangular waveform with amplitude somewhat higher than the coercivity of the core, so that the signal can, periodically, switch the core between its (stable) steady states. The signal frequency is, typically, determined by the desired data collection rate as well as other core characteristics (which usually determine the sensor bandwidth).

Saturation leads to a change in the core relative permeability and, hence, the output voltage. With an applied time-periodic excitation and the absence of a dc target signal, the response (measured in the pickup coil) is a periodic bistable rectangular signal; a power spectral density (PSD) calculated for this output has harmonics at the odd multiples of the excitation frequency due to the structure of the nonlinearity, as predicated by stability requirements. An external dc magnetic field breaks the symmetry of the voltage output, leading to the appearance of all harmonics of the driving signal in the PSD. This asymmetry induced behavior is the hallmark of a dc perturbation signal.

The detection of a dc target signal via the second harmonic component of the sensor output voltage is the traditional and the most studied [10], [11], [12], [33], [34], [35], [36] technique, relying on a calculation of the amplitude of the second harmonic in the PSD of the output voltage (in the secondary or pickup coil) [11], [12], [37]. It was, traditionally, believed [28], [34], [38] that the second harmonic detection method had the best performance (benchmarked by low noise and high stability), however Ripka [39], affirmed that the second harmonic detection technique required an excitation current without higher harmonic distortion, and the readout circuitry should include at least a band-pass filter, a phase-sensitive detector, and an integrator. Hence, considering the usual criteria, e.g., low power, low cost, and simplicity, other techniques might well be preferable. One of these techniques is the "peak detection" or RTD method [7], [8], [9].

The RTD method exploits the asymmetry of the voltage output caused by an external dc magnetic field in the time domain. Without an external dc field, the symmetric periodic excitation current leads to a periodic saturation of the core alternating equally positive and negative magnetization. The essence of the technique is to measure the switching times at which transitions between the steady states occur, thereby yielding a calculation of the "residence times" in each stable state. In the absence of the asymmetrizing dc signal, the mean residence time *difference* is zero; in the presence of the dc signal, the potential energy function is skewed, the system spends unequal times in the steady states and the mean RTD is nonzero and proportional to the dc target signal. The method is simple to implement, usually requiring a clock-counter mechanism to record switching events while maintaining a running average (because of the background noise), and a theoretical calculation of the mean RTD can be carried out and shown to match experimental observations very well [30]. We note, in passing, that a more rigorous theoretical analysis, based on a computation of the Shannon information transfer in a bistable sensor also has demonstrated that the RTD appears to yield more accurate signal estimation than the FFT (which underpins the second harmonic readout); in particular, the RTD does not have the issue of loss of information due to the mixing phenomena that occur in the FFT [40].

The internal noise in a fluxgate magnetometer can be caused by several factors: perm or remanent effect caused by nonuniformity of the core or nonuniform magnetization, thermal noise depending on the coil mass and diameter [38], or mechanical stress. Non3uniform magnetization can arise from inhomogeneities in the windings or by nonuniformity of the external magnetic field. Most of the causes of internal noise are similar to those causing the demagnetizing effect [38]. Primdahl et al. [24] demonstrated the dependence of the internal noise on the demagnetizing factor, and modeled it as an equivalent external noise linked to D

$$B_n = \mu_0[1 + D(\mu_r - 1)]h_n \cong \mu_0\mu_r D h_n = D b_n \qquad (1)$$

with μ_0 being the permeability of the open space, b_n being the internal induction noise field, B_n being the equivalent external induction noise field, and h_n being the internal noise field.

In the same manner, for the RTD fluxgate, the noise fluctuations generated in the core are estimated to be [29]

$$H_n = D\mu_r h_n \qquad (2)$$

with H_n being the equivalent external noise field. In fact, in the RTD analysis, the $H - field$ must be taken into account instead of the $B - field$. The dependence on the demagnetizing factor is the same for both the readouts. Thus, the reduction of internal noise is independent of the readout; the noise reduction can, however, be achieved through a different geometry. Gordon et al. [41] confirmed that a closed core structure is preferable to an open one due to the better magnetization of the core and the absence of free ends. This is intuitively clear because inhomogeneities in the magnetization of the core and the perm effect are the main sources of noise. In fact, the internal demagnetizing factor in a closed core is lower than the open core. So, the race-track is a tradeoff between low demagnetization and the strengths of a closed core structure [28].

Another source of noise is thermal noise caused by the coil [38]: it affects the voltage output and depends on the coil mass and diameter; most importantly, the RTD readout is independent of the amplitude of the voltage output because it only depends on the residence times, meaning an intrinsic independence of the output from thermal noise. The lower effect of noise on the voltage output instead might be useful from a power consumption standpoint: a less noise-influenced voltage amplitude means a lower current amplitude required in the coil assuring similar performances in the two readouts. It is worth mentioning that the amplitude of the bias signal can be taken to be far lower when one uses the RTD readout, compared with the second harmonic readout in a magnetometer using the same core structure/geometry. This can result in a significant power saving, and a smaller level of noise emanating from the signal generator. Other noise sources have been discussed in [18], [24], and [42].

III. PROPOSED HORSESHOE STRUCTURE

One of the major problems associated with the fluxgate magnetometer is the reliability of the measurements when the system is operated in an unshielded environment; since the sensor is usually dealing with very small magnetic targets, it is also very sensitive to any external (unwanted) magnetic disturbance. In an open core, such as the rod core, the flux lines of the biasing field inside the fluxgate interact far more easily with the flux lines of other magnetic sources. Therefore, the sensor is really sensitive to its location/position and to any perturbation in the external environments; hence, measurements in unshielded environments are difficult. Primdahl [12] has also demonstrated that in an open core structure the flux lines of the biasing field inside the fluxgate tend to close through a metal object in its proximity, leading to a higher susceptibility to variation of the environment, as well as a higher demagnetization than the closed core. Thus, a different structure with a different sense mechanism has been developed.

The coupled fluxgate structure proposed in this work is a horseshoe configuration similar to a racetrack, but with an air gap at the north end (see Fig. 1). This sensor is used here to perform measurements on a target placed in proximity to the air gap. The horseshoe configuration is obtained by connecting in series three flexible microwire fluxgates [43] through their excitation coil and their core; this topology is intended to maintain high sensitivity to the target signal while attenuating the effects of noise, demagnetization, and other spurious external magnetic disturbances. Each flexible microwire fluxgate is made up of a CoFeSiB microwire

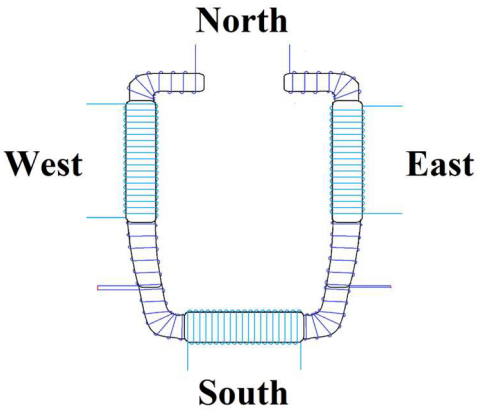

FIGURE 1. "Horseshoe-coupled" RTD fluxgate magnetometer.

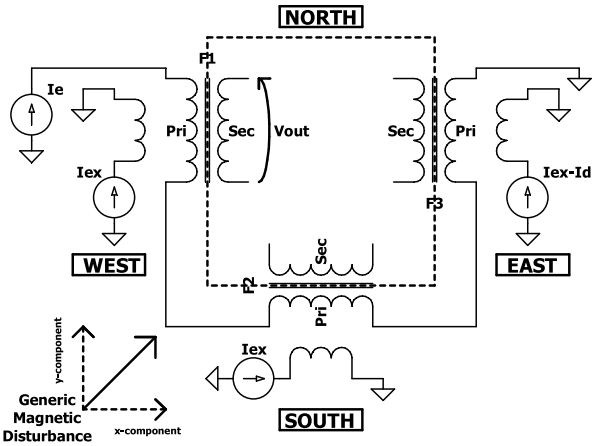

FIGURE 2. Horseshoe configuration model.

surrounded by 900 turns of a copper filament as excitation coil and, only in the center section, by 900 turns of a 4-layer copper wire serving as the pick-up coil. Each sensor length is about 12 cm [43]. The CoFeSiB microwires of the Horseshoe Configuration are connected in series by direct contact: one end of the West fluxgate is in contact aligned with the end at west of the South fluxgate and the end at east of the South fluxgate is in contact aligned with one end of the East fluxgate. The flexibility of the microwire arouses interest considering that it allows the bending of the microwire ends and, hence, the connection in series of the cores. Moreover, the flexibility determines a (smooth) curvature and not a sharp corner at each bend, avoiding magnetostriction. By positioning the two free ends of the core pointing each other and with a very small separation (∼5 cm), a preferential return path for the flux lines is assured. The result is a pseudo-racetrack with the benefits of the classical racetrack (low demagnetization, low cross-field, and low noise) [41], [44] slightly reduced because of the presence of the air gap, but with better performances than the single-rod geometry. In this way, spatial selectivity typical of the rod type [43], [45] and closing of the flux lines are both guaranteed. Most importantly, however, the horseshoe structure can be used as an input differential device to shield it from external stochastic disturbances. It is impossible to use a magnetic shield covering the device because it could also shield it from the target magnetic field. Instead, through this structure, the device is internally shielded: the same external magnetic field has a different effect on the two branches of the structure, additive on the excitation field of one branch and subtractive on the excitation field of the other. So, the two effects compensate each other.

The air gap or the region at the open end of the horseshoe is functional to sensing the target. In fact, despite the air gap, the flux lines of the magnetic field biasing the core are closed and cross the target, so the presence of the target in the middle of the air gap causes a variation of the reluctance of the device, similar to an inductive sensor. The variation of the reluctance determines a variation in the $H-$field, so that the excitation field H_e becomes

$$H_{e_{\text{tot}}} \cong H_e \cdot \frac{1}{1+\frac{d(1-\mu_r)}{l+\mu_r h}} \tag{3}$$

where $H_{e_{\text{tot}}}$ is the total magnetic field in the whole structure, H_e is the magnetic field without the presence of the iron samples, d is the length of the flux line path covered by the iron samples, l is the length of the core, and h is the length of the air gap (we are assuming samples and core having about the same relative permeability). The RTD readout was used in this work because of all the advantages already discussed earlier.

The typical electrical model of the fluxgate is the transformer [39]. The three fluxgates connected in series were modeled as three transformers (see Fig. 2): the primaries of the transformers are the excitation coils, which are connected in series with the current flowing in the same direction for all of them; the secondaries of the transformers are the pick-up coils and only one of them is exploited. The external disturbance was modeled for each transformer as a current source I_{ex} connected to a primary in parallel to the primary determined by the excitation coil (through which flows the biasing current I_e); this primary generates a flux that is added to the excitation flux and sensed by the secondary. The direction of the current at East and West simulate the direction of the uniform magnetic flux acting on the fluxgate. In fact, because of the high spatial selectivity of the single fluxgate [43], each fluxgate senses above all only the component of the external disturbance in parallel with its own core.

Also, the distance with respect to the disturbance source must be taken into account, therefore, in the case of an S-W disturbance like in Fig. 2, the value of the current generated at East is corrected by a factor I_d effectively reducing the amplitude of the magnetic disturbance.

In this article, our experimental activity has been developed to help diagnose neurodegenerative diseases via the increase in iron concentration in the basal ganglia that accompanies the disease. In previous works [17], [46], the

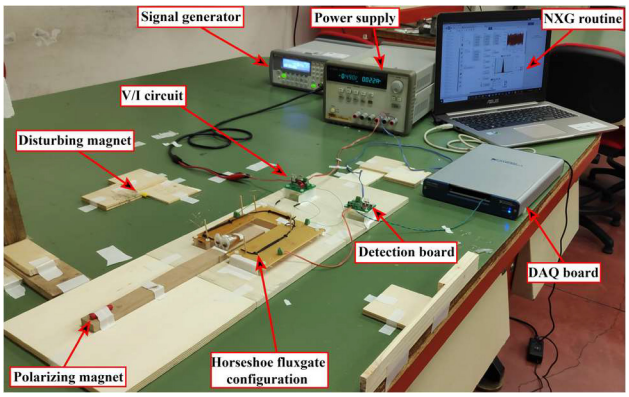

FIGURE 3. Experimental setup (see text).

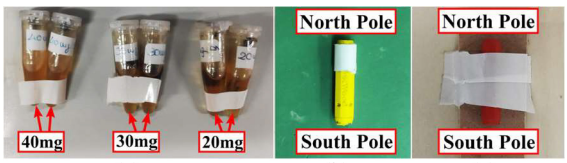

FIGURE 4. (a) Ferrofluidic samples used in the measurements (40, 30, and 20 mg). (b) Disturbing magnet. (c) Polarizing magnet.

capability of this sensor to detect iron compounds up to 5 mg has been experimentally demonstrated, with an experimental resolution of about 2 mg. As described before, the horseshoe sensor presented in this article has its sensing region in the gap between the two ends, along the magnetic path. In view of this application, the sensor must cover all the head semicircumference in order to have the target (basal ganglia) between the two free ends.

This structure can allow the integration of the sensor into a specially designed helmet, rendering the whole system portable.

IV. EXPERIMENTAL SETUP

The experimental setup (Fig. 3) consists of the following.

1) The system previously described in which the output voltage is picked up from only one fluxgate.
2) Samples with different concentrations (20, 30, and 40 mg) of ferromagnetic material dispersed in oil (used in the experimental setup of the previous works [17], [46]) as targets [Fig. 4(a)].
3) A permanent magnet (yellow) (length of 2.5 cm, diameter of 0.5 cm, generating a static magnetic field of about 40 μT evaluated at 5 cm of distance) to simulate the external disturbance at different directions [Fig. 4(b)].
4) A permanent magnet (red) (the same as the previous) to magnetize the iron compounds [Fig. 4(c)].
5) A V/I converter to provide the current to the excitation coils connected in series from the signal generator.
6) A readout circuit made up of a differential amplifier and a trigger to convert the signal output into a square waveform.
7) A DAQ board (NI USB-6366) for the acquisition of the signal from the readout circuit.
8) A signal generator (Keysight 33220A) to provide a sinusoidal voltage at specific amplitude and frequency to the V/I converter, in this case a sinusoidal voltage having an amplitude of 200 mVpp (current of 2 mApp) and a frequency of 60 Hz, in accordance with the optimal condition previously found [32].
9) A power supply (Agilent E3631A) for the V/I converter and the readout circuit.

The current is imposed through the V/I converter at one excitation coil's terminal of the East fluxgate and one excitation coil's terminal of the West one; the remaining two terminals are connected to the excitation coil of the fluxgate in the middle (South fluxgate). In this way, the current is the same along the three fluxgates, so the variable magnetic field produced in each of them is also the same. Moreover, also the three cores are connected, in fact the core of the South fluxgate is in contact aligned at left with the West fluxgate's core and at right with the East one. In this way, ideally, the three fluxgates will have exactly the same magnetic field (not only the excitation field) in the three cores, thereby making the entire setup behave like a single fluxgate. This allows for the compensation of the external disturbance. Finally, the output voltage is drawn from only one fluxgate's pick-up coil.

This new configuration has been compared to the single fluxgate with an end folded at 90° to better understand differences, strengths, and weaknesses. To minimize alteration of the measurement due to the changing environment between the two configurations, the West fluxgate of the Horseshoe configuration has been used to test the single folded one, connecting the V/I converter only to its excitation coil and disconnecting its core from the South fluxgate, like a mechanical switch [Fig. 5(c)]. In fact, the West fluxgate and the East fluxgate of the Horseshoe configuration are both with the free end folded at 90° in order to point each other. In this way, it has been possible to test two different configurations [Fig. 5(a) and (b)], both folded, through a unique structure.

V. RESULTS

The purpose of the measurements consists in the evaluation of the Horseshoe configuration performances, and the comparison with those of a single fluxgate, when an external disturbing magnetic field is present in addition to a metal-based target presented to the fluxgate.

A. DISTURBANCE ATTENUATION: HORSESHOE VERSUS SINGLE FLUXGATE

Each sample of the target is placed between the free ends of the cores. The red magnet points to the sample to polarize it while the yellow magnet directly points to the Horseshoe configuration at a distance of 17.5 cm (to implement a magnetic disturbance) (Fig. 6).

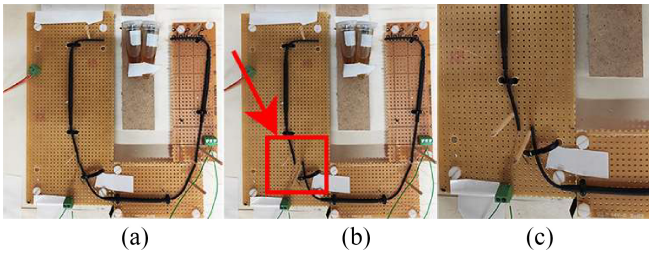

FIGURE 5. (a) Horseshoe Configuration. (b) Single Configuration obtained from the Horseshoe. (c) Zoom on the pseudo mechanical switch used to switch between the two configurations.

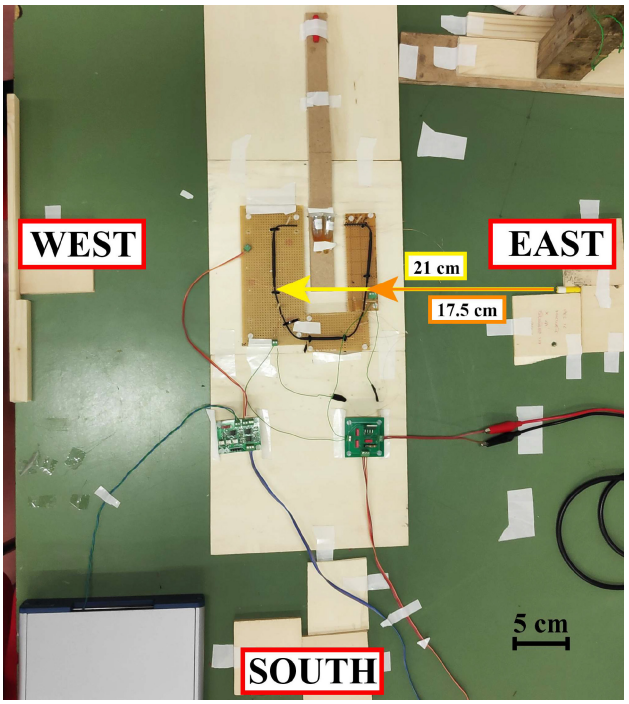

FIGURE 6. Experimental setup focused on the three possible different positions of the disturbing magnet (West, East, and South).

For each configuration, five measurements were carried out: 1) without samples; 2) with samples; 3) with samples and a magnetic disturbance at West; 4) with samples and a magnetic disturbance at South; and 5) with samples and a magnetic disturbance at East.

Each measurement was carried out in the presence of the polarizing magnet (red). The measures in the presence of the disturbance have been performed for each polarity of the disturbing magnet (yellow), South pole and North pole.

Moreover, the measurements have been carried out maintaining fixed the position of the samples, so conducting for each sample all the measurements for one configuration and then for the other one. This method determines a change of the initial conditions, so it is impossible to estimate the sensitivity. The sensitivity has been estimated through the third set of measurements (Section V-C).

Differently than usual, when trigger and offset are both adjusted to obtain the RTD as close as possible to zero in

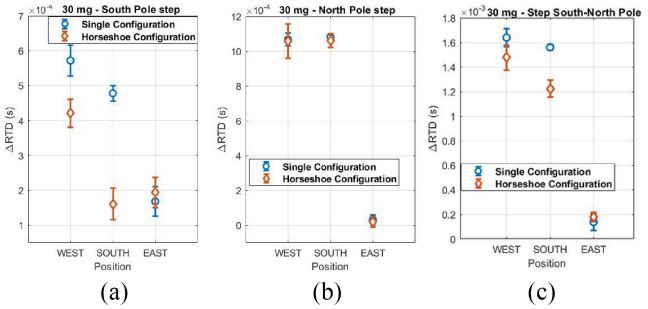

FIGURE 7. Δ(RTD) between the two readings in presence and in the absence of disturbances [(a) South pole or (b) North pole] and (c) Δ(RTD) between the two readings in presence of a South pole disturbance and a North pole disturbance.

the absence of the target and, therefore, a duty cycle of about 50%, in this experiment, the duty cycle was adjusted at about 47% to allow visualizing the disturbance polarity.

A quantitative analysis has been conducted through the estimation of the ΔRTD between the two readings in presence (South or North pole) and in the absence of disturbances and between the two readings in presence of a South pole disturbance and in presence of a North pole disturbance. For each measure, the ΔRTD mean value and the standard deviation have been evaluated using time-windows of about 4 s. The results have been plotted versus the position of the disturbance with their uncertainty band at $\pm 3\sigma$, σ being the standard deviation. In this work, the results for 30 mg have been shown since changing the concentrations does not, qualitatively, change the results. The complete analysis is presented in [32].

Fig. 7(a) shows that the Horseshoe configuration has a better response (a smaller change in RTD) to South pole disturbance than the single one ($4.2 \cdot 10^{-4}$ s versus $5.7 \cdot 10^{-4}$ s with a West disturbance and $1.6 \cdot 10^{-4}$ s versus $4.7 \cdot 10^{-4}$ s with a South disturbance). In general, the Horseshoe configuration has the advantage of a better response to slowly varying magnetic field compared to the single one [Fig. 7(c)]. In this case, the better response is represented by a smaller change in RTD (ΔRTD) because the magnetic field sensed by the two configurations is simulating an external magnetic disturbance and the purpose of this work is to maximize the immunity to it. Only in the case of a disturbance acting at East position, the Horseshoe configuration output is equivalent to the single configuration or worse because the Horseshoe structure is closer to the disturbing magnet (17.5 cm) than the single structure (21 cm) (Fig. 6).

The advantage of using the horseshoe-coupled fluxgate to reduce the unwanted effects of external disturbances is therefore clear.

B. DISTURBANCE ATTENUATION AND OPTIMAL OUTPUT VOLTAGE

The architecture of the horseshoe-coupled fluxgate allows for consideration of a nulling effect due to the differential interaction of the two parallel branches, this differential effect should appear enhanced in the South fluxgate (thanks to the

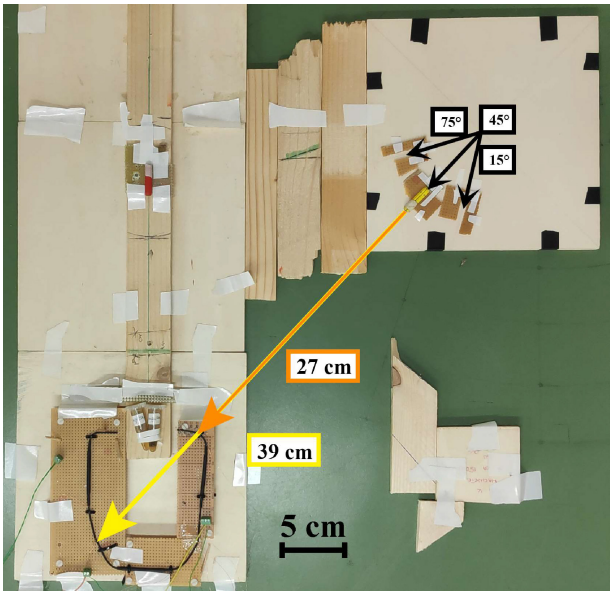

FIGURE 8. New positions of the disturbing magnet (angle of 15°, 45°, and 75°).

symmetry of the structure); that is, therefore, the one to be considered as the candidate for reading the optimal output voltage. Some further measurements have been performed to validate this concept by using a perturbing magnet placed at 15°, 45°, and 75° (see Fig. 8).

The raw signal of the RTD for the three configurations with the disturbance at 45° is plotted in Fig. 9(a). Instead, the overall results are plotted in Fig. 9(b) as variation of RTD between the value obtained in the absence and presence of disturbance. Each ΔRTD mean value has been evaluated using time windows of about 5 s.

Also in this case, the better response is represented by a smaller change in RTD (ΔRTD) because the magnetic field sensed by the three configurations is simulating again an external magnetic disturbance. At 45°, the U-South has a better response ($\sim 6.86 \cdot 10^{-4}$ s) than the U-West ($\sim 8.25 \cdot 10^{-4}$ s) and the single configuration ($\sim 7.63 \cdot 10^{-4}$ s). At 45°, the disturbance is exactly the same for the U-South and the U-West, so the better response of the U-South than the U-West confirms the assumptions from the previous set of measurements, that is, the structure is effectively acting in a differential way against the external magnetic field and the South fluxgate is the best option because it exploits the two fluxes from the West and the East fluxgate, which sense the external field exactly in opposite directions. For the same reason as the previous measurement, the U-West is worse than the single configuration. This is also coherent with the noncomplete compensation due to some nonidealities, such as cores not exactly aligned. The microwires are really thin (100 μm), so it is impossible to match two free ends exactly. The consequence is a flux leakage greater the less aligned is the contact of the microwires' ends. For this reason, the compensation of the external disturbance is not total. Moreover, the compensation cannot be total because the magnetic disturbance is closer to the East fluxgate than

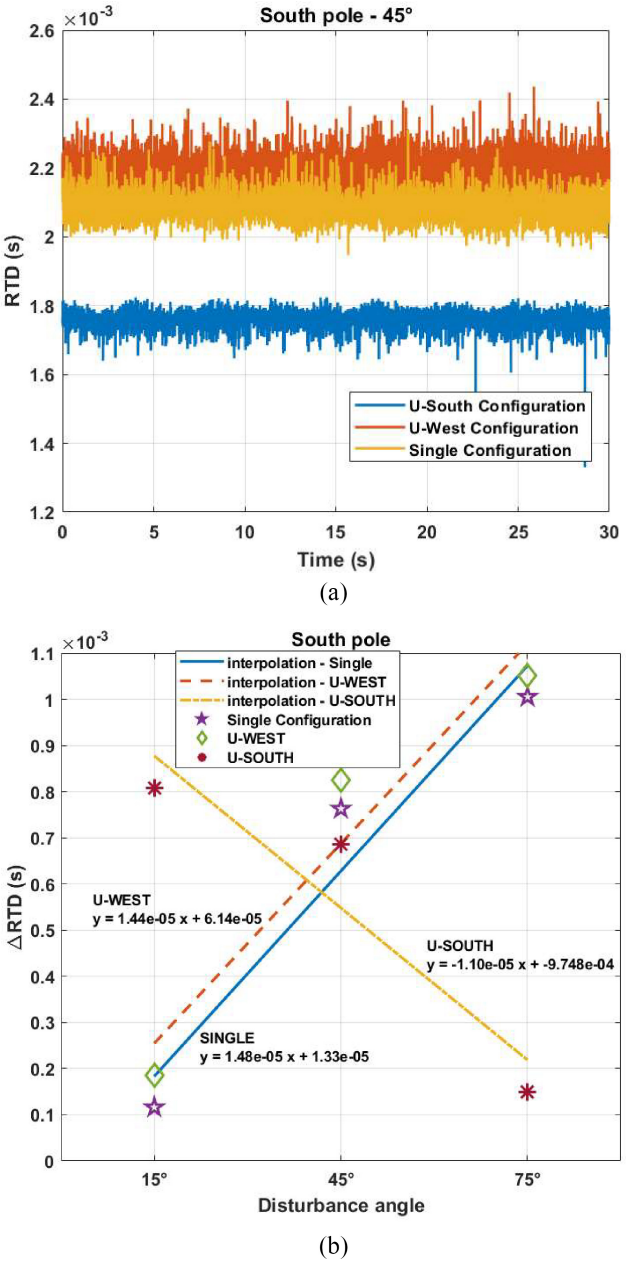

FIGURE 9. Response of the three configurations (Single, U-West and U-South). (a) Raw signal of the RTD for a disturbance at 45°. (b) ΔRTD by varying the angle of the disturbing magnet (external magnetic disturbance).

the West fluxgate, so the flux inside the two branches is not exactly the same. This is a confirmation of the model in Fig. 2. In general, the maximum magnetic disturbance sensed by the Horseshoe structure in this experimental setup is 0.4 μT (static magnetic field of the permanent magnet at 27 cm of distance).

The results at 15° and 75° are unexpected: despite being part of the Horseshoe structure, the fluxgates keep their spatial selectivity [43], in fact the U-South gives higher variation to a disturbance at 15° than a disturbance at 75° because the South fluxgate end is more in line with the first than the latter. Similarly, the U-West and the single gives higher

variations to a disturbance at 75° than a disturbance at 15° because the West fluxgate is more in line with the disturbance at 75°. This result seems to go against the previous assumption, but it is not: it confirms the nonidealities and it shows that, despite all this, the U-South has a lower vectoriality than the U-West and the single fluxgate. In fact, linear interpolation in Fig. 9(b) shows a smaller slope of the U-South than the U-West and the single.

Another important result obtained through this set of measurement is the comparison of the RTD standard deviation at zero target between the three configurations: the U-South has the lowest RTD standard deviation at zero target ($7.04 \cdot 10^{-6}$ s) and the single fluxgate has the highest ($1.261 \cdot 10^{-5}$ s). The noise level can be estimated starting from the standard deviation of the RTD estimated in the absence of the target [29], [43], so the U-South has the lowest noise level and the single fluxgate has the highest, as expected.

C. RESPONSIVITY

The previous measurements clarify that the U-South is the best configuration for disturbance attenuation, so the following measurements have been focused only on sensing with this configuration.

In order to estimate responsivity of this sensor, the same experimental setup of the other two types of measurements has been used, but without the disturbing magnet. Three different contents of ferromagnetic material have been used: 1) 20 mg; 2) 30 mg; and 3) 40 mg [Fig. 4(a)].

Three types of measurements have been carried out.

1) Without polarizing magnet and iron compounds.
2) With only the polarizing magnet.
3) With the polarizing magnet and the iron compounds placed by turn into the gap.

The polarizing magnet was placed at 18 cm from the target.

Analyzing the results obtained polarizing through the South pole (Fig. 10), the sensitivity (estimated through a linear interpolation) is about 8.17 μs/mg and the RTD maximum uncertainty is about $9.14 \cdot 10^{-6}$ s with a time window of 5 s.

These results can be compared with the results obtained in [32] because the measurements were carried out in the same working point (optimal frequency—current amplitude couple, south-pole polarization, and fluxgate bended, so same magnetostriction and so on). In [32], the focus is on the results for the smaller iron compounds (from 0 to 10 mg), but the measurements were carried out for the whole range from 0 to 50 mg. The results between 20 and 40 mg have been extrapolated (Fig. 11) obtaining a sensitivity (estimated through a linear interpolation) of 5.77 μs/mg and an RTD maximum uncertainty of $3.99 \cdot 10^{-6}$ s with a time windows of 5 s. The uncertainty is different because these measurements were carried out in a less noisy environment. Moreover, in [32], it is clearly explained that the sensitivity to the smaller iron compounds is higher than the sensitivity

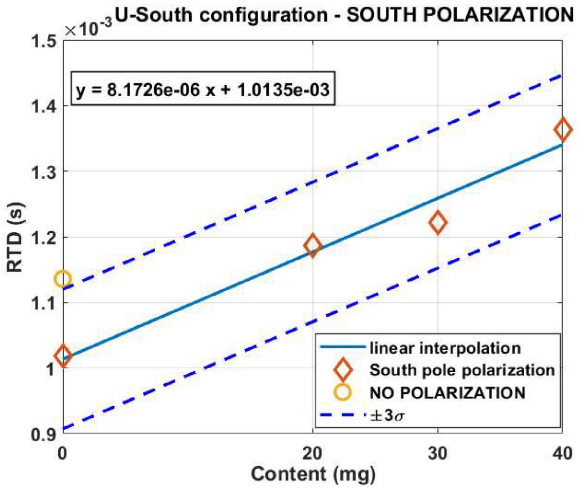

FIGURE 10. U-South sensitivity: interpolation of the response with South pole polarization.

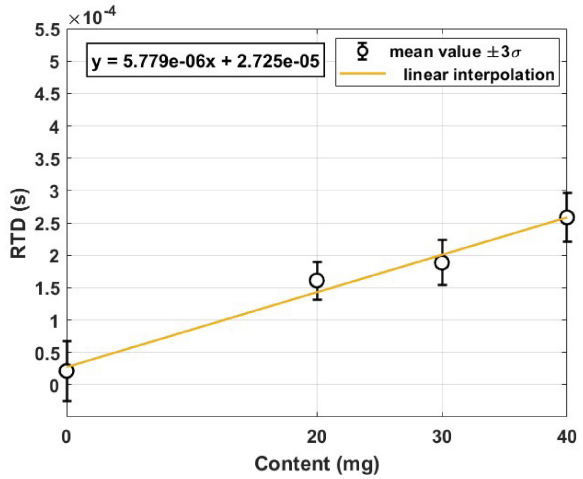

FIGURE 11. Single fluxgate sensitivity from [32] focused only on the iron content between 20 and 40 mg.

to the larger one because of the saturation of the core, so the sensitivity of the U-South is expected to be even higher than 8.17 μs/mg for smaller iron compounds.

This is an important result because it confirms the lower demagnetizing effect due to closing the flux lines. Furthermore, it confirms an important advantage of the RTD readout: the sensitivity does not depend on the direction of the pick-up coil with respect to the target, as the second-harmonic readout does [10], [34], because the vectoriality of the single rod [43] is preserved. Thus, the U-South structure reduces the sensitivity (ΔRTD) to the external magnetic field and increases the sensitivity to the target inside the air gap.

D. SOUTH VERSUS NORTH POLARIZATION

The application of a South pole magnetic field has, in general, a different effect on the fluxgate with respect to a North pole magnetic field.

The duty cycle of the output waveform cannot ever be set exactly at 50% because of fluctuations caused by the noise so, in general, it is preferable to set the duty cycle far from

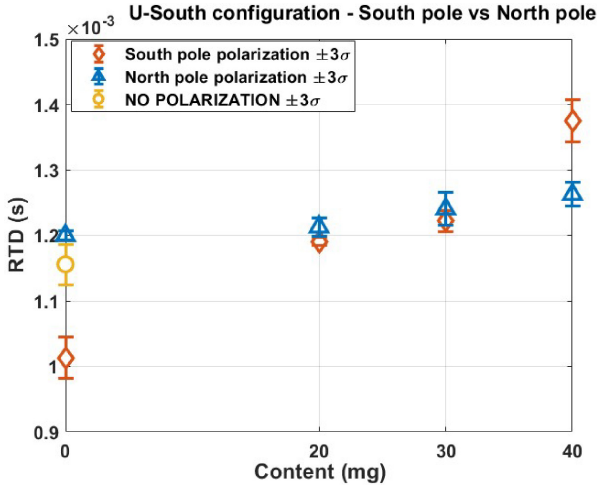

FIGURE 12. U-South sensitivity: comparison between the response with South pole polarization and North pole polarization of the target.

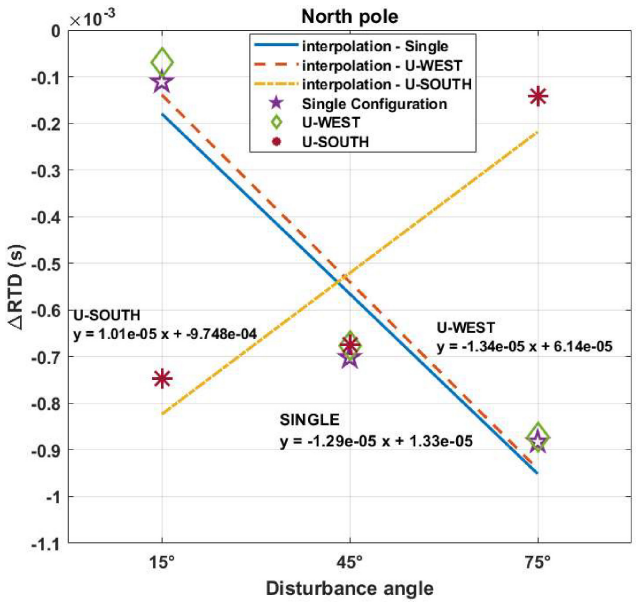

FIGURE 13. Response of the three configurations (Single, U-West, and U-South) by varying the angle of the disturbing magnet (external magnetic disturbance) for a North pole disturbance.

this point because it is a source of uncertainty of the measure (the RTD is calculated as an absolute value with respect to the 50% threshold [32]). For this reason, the sensor saturates earlier for one magnetic field polarity than the other, so the response of the fluxgate is different according to the external magnetic field polarity.

Fig. 12 confirms different sensitivity of the sensor to a target magnetized with a North pole magnetic field with respect to the South one. The Horseshoe structure determines the reduction of the vectoriality (Fig. 13) and the reduction of the noise also for a North pole disturbance with respect to the single configuration (Table 1).

So, the benefits of the Horseshoe configuration are guaranteed regardless of the polarity of the external magnetic disturbance.

TABLE 1. Comparison between the three configurations.

	U-South	U-West	Single
Slope North pole ($^S/_\circ$)	$1.01 \cdot 10^{-5}$	$1.34 \cdot 10^{-5}$	$1.29 \cdot 10^{-5}$
Slope South pole ($^S/_\circ$)	$1.10 \cdot 10^{-5}$	$1.44 \cdot 10^{-5}$	$1.48 \cdot 10^{-5}$
Noise level (s)	$7.04 \cdot 10^{-6}$	$1.251 \cdot 10^{-5}$	$1.261 \cdot 10^{-5}$

VI. CONCLUSION

In this work, the Horseshoe configuration is presented for fluxgate magnetometers with the aim of obtaining a measurement system with high immunity to external spurious magnetic fields. This configuration combines the low internal demagnetizing field thanks to the quasi closed-flux geometry, and the low external demagnetizing field thanks to the straight branch similar to a racetrack. The lower (overall) demagnetizing effect assures lower noise, as demonstrated in the literature.

Three fluxgates with cores and excitation coils in series are used to emulate a single long rod fluxgate folded in the shape of a horseshoe. The sensing is performed in the gap between the two free ends exploiting both the variation of the reluctance inside the closed-loop flux lines and the vectoriality of the rod fluxgate to sense the target magnetic field. The magnetic field external to the gap is theoretically nullified through the two horseshoe branches pointing their cores in opposite directions to the other one (because of the series configuration) (Fig. 2).

The results clearly show the enhancing of the immunity to the external disturbances (ΔRTD of $\sim 6.86 \cdot 10^{-4}$ s for the U-South) with a contemporary increase of responsivity (sensitivity to the target of 8.17 μs/mg for the U-South) with respect to the single rod RTD fluxgate (Δ RTD caused by an external disturbance of $\sim 7.63 \cdot 10^{-4}$ s and sensitivity to the target of 5.77 μs/mg).

The noise affecting the sensor has been evaluated starting from the standard deviation of the RTD estimated in the absence of a target. Hence, a comparison between the three structures at identical conditions has been possible. As expected from the above, the U-South has the lowest standard deviation and the single fluxgate has the highest one ($7.04 \cdot 10^{-6}$ s for the U-South and $1.261 \cdot 10^{-5}$ s for the single configuration), so the Horseshoe configuration is less affected by noise.

However, another important result can be extrapolated from this study: using the RTD readout, the sensitivity does not depend on the direction of the pick-up coil with respect to the target as in the second harmonic readout, but it only depends on the position of the fluxgate's ends. This is an important result because it allows the folding of the fluxgate according to the application field and it paves the way to new theoretical analysis about the "effective path length" of the external magnetic field in an RTD fluxgate, and then about the demagnetization.

ACKNOWLEDGMENT

The authors thank Dr. Valentina Sinatra for her support regarding the fluxgate and the development of the experimental setup.

REFERENCES

[1] M. Acuna, "Fluxgate magnetometers for outer planets exploration," *IEEE Trans. Magn.*, vol. 10, no. 3, pp. 519–523, Sep. 1974.

[2] M. H. Acuna, C. Scearce, J. B. Seek, and J. L. Scheifele, "The MAGSAT vector magnetometer: A precision fluxgate magnetometer for the measurement of the geomagnetic field," document NASA-TM-79656, NASA, Washington, DC, USA, 1978.

[3] P. Ripka, "Improved fluxgate for compasses and position sensors," *J. Magnetism Magnet. Mater.*, vol. 83, no. 1, pp. 543–544, 1990.

[4] P. Brauer, T. Risbo, J. Merayo, and O. Nielsen, "Fluxgate sensor for the vector magnetometer onboard the 'Astrid-2' satellite," *Sens. Actuators A, Phys.*, vol. 81, no. 1, pp. 184–188, 2000.

[5] J. Tomek, A. Platil, P. Ripka, and P. Kaspar, "Application of fluxgate gradiometer in magnetopneumography," *Sens. Actuators A, Phys.*, vol. 132, no. 1, pp. 214–217, 2006.

[6] M. Janosek, P. Ripka, and A. Platil, "Magnetic markers detection using PCB fluxgate array," *J. Appl. Phys.*, vol. 105, no. 7, 2009, Art. no. 7E717.

[7] A. R. Bulsara, C. Seberino, L. Gammaitoni, M. F. Karlsson, B. Lundqvist, and J. W. C. Robinson, "Signal detection via residence-time asymmetry in noisy bistable devices," *Phys. Rev. E, Stat. Phys. Plasmas Fluids Relat. Interdiscip. Top.*, vol. 67, no. 1, 2003, Art. no. 16120.

[8] B. Andò, S. Baglio, A. Bulsara, V. Caruso, and S. Castorina, "A new readout strategy for fluxgate sensor," in *Proc. 20th IEEE Instrum. Technol. Conf.*, vol. 1, 2003, pp. 600–604.

[9] B. Andò, S. Baglio, A. R. Bulsara, and V. Sacco, "'Residence times difference' fluxgate magnetometers," *IEEE Sensors J.*, vol. 5, no. 5, pp. 895–904, Oct. 2005.

[10] A. W. Geyger, "The ring-core magnetometer 'A new type of second-harmonic flux-gate magnetometer,"' *Trans. Amer. Inst. Electr. Eng. I, Commun. Electron.*, vol. 81, no. 1, pp. 65–73, Mar. 1962.

[11] S. V. Marshall, "An analytic model for the fluxgate magnetometer," *IEEE Trans. Magn.*, vol. 3, no. 3, pp. 459–463, Sep. 1967.

[12] F. Primdahl, "The fluxgate mechanism, part I: The gating curves of parallel and orthogonal fluxgates," *IEEE Trans. Magn.*, vol. 6, no. 2, pp. 376–383, Jun. 1970.

[13] B. Andò et al., "A novel measurement strategy for volcanic ash fallout estimation based on RTD fluxgate magnetometers," in *Proc. IEEE Instrum. Meas. Technol. Conf.*, 2008, pp. 1904–1907.

[14] C. Trigona, V. Sinatra, A. R. Fallico, S. Puglisi, B. Andò, and S. Baglio, "Dynamic spatial measurements based on a bimorph artificial whisker and RTD-fluxgate magnetometer," in *Proc. IEEE Int. Instrum. Meas. Technol. Conf. (I2MTC)*, 2019, pp. 1–5.

[15] P. Lipovský, M. Fil'ko, J. Novotňák, Z. Szöke, M. Košuda, and K. Draganová, "Concept of magnetic microwires based magnetometer for UAV geophysical survey," in *Proc. New Trends Signal Process. (NTSP)*, 2020, pp. 1–5.

[16] G. Caposciutti, M. Marracci, C. Trigona, S. Baglio, and B. Tellini, "Investigation of a 100 μm magnetic wire for temperature sensing based on a time domain readout," in *Proc. IEEE Int. Instrum. Meas. Technol. Conf. (I2MTC)*, 2021, pp. 1–6.

[17] C. Trigona et al., "Measurements of iron compound content in the brain using a flexible core fluxgate magnetometer at room temperature," *IEEE Trans. Instrum. Meas.*, vol. 67, no. 4, pp. 971–980, Apr. 2018.

[18] D. Scouten, "Sensor noise in low-level flux-gate magnetometers," *IEEE Trans. Magn.*, vol. 8, no. 2, pp. 223–231, Jun. 1972.

[19] D. M. Miles et al., "Low-noise permalloy ring cores for fluxgate magnetometers," *Geosci. Instrum., Methods Data Syst.*, vol. 8, no. 2, pp. 227–240, 2019.

[20] D. Gordon, R. Lundsten, and J. Scarzello, "Offset and noise in fluxgate magnetometers," *IEEE Trans. Magn.*, vol. 6, no. 4, p. 818, Dec. 1970.

[21] O. V. Nielsen et al., "Analysis of a fluxgate magnetometer based on metallic glass sensors," *Meas. Sci. Technol.*, vol. 2, no. 5, pp. 435–440, 1991.

[22] P. Ripka, M. Butta, F. Jie, and X. Li, "Sensitivity and noise of wire-core transverse fluxgate," *IEEE Trans. Magn.*, vol. 46, no. 2, pp. 654–657, Feb. 2010.

[23] M. Butta, P. Ripka, and J. Kubik, "Algorithm for noise reduction in output signal of race-track core fluxgate," *PIERS Online*, vol. 3, pp. 1307–1310, Jan. 2007.

[24] F. Primdahl, B. Hernando, O. V. Nielsen, and J. R. Petersen, "Demagnetising factor and noise in the fluxgate ring-core sensor," *J. Phys. E, Sci. Instrum.*, vol. 22, no. 12, pp. 1004–1008, 1989.

[25] F. Primdahl, P. Ripka, J. R. Petersen, and O. V. Nielsen, "The sensitivity parameters of the short-circuited fluxgate," *Meas. Sci. Technol.*, vol. 2, no. 11, pp. 1039–1045, 1991.

[26] C. Hinnrichs, J. Stahl, K. Kuchenbrandt, and M. Schilling, "Dependence of sensitivity and noise of fluxgate sensors on race-track geometry," *IEEE Trans. Magn.*, vol. 37, no. 4, pp. 1983–1985, Jul. 2001.

[27] E. Özkök, H. Can, F. İnanır, and U. Topal, "A comparative study for optimization of sensitivity and noise levels in race-track sensors," *J. Supercond. Novel Magnetism*, vol. 30, no. 12, pp. 3555–3557, 2017.

[28] P. Ripka, "Advances in fluxgate sensors," *Sens. Actuators A, Phys.*, vol. 106, nos. 1–3, pp. 8–14, 2003.

[29] B. Andò, S. Baglio, A. R. Bulsara, V. Caruso, V. In, and V. Sacco, "Investigate the optimal geometry to minimize the demagnetizing effect in RTD-fluxgate," in *Proc. IEEE Instrum. Meas. Technol. Conf.*, 2006, pp. 2175–2178.

[30] A. R. Bulsara et al., "Exploiting nonlinear dynamics in a coupled-core fluxgate magnetometer," *Meas. Sci. Technol.*, vol. 19, no. 7, 2008, Art. no. 75203.

[31] F. Antoci et al., "Injection locking in coupled core fluxgate magnetometers: Exploiting nonlinearity to enhance sensitivity to weak, low frequency, target magnetic fields," *IEEE Sensors J.*, vol. 14, no. 2, pp. 554–562, Feb. 2014.

[32] C. Ferro, "Development and characterisation of innovative measurement systems for non-invasive diagnosis of neuroferritinopathies based on fluxgate magnetometers," M.S. thesis, Dipartimento di Ingegneria Elettrica Elettronica e Informatica, Univ. Catania, Catania, Italy, 2021.

[33] J. Burger, "The theoretical output of a ring core fluxgate sensor," *IEEE Trans. Magn.*, vol. 8, no. 4, pp. 791–796, Dec. 1972.

[34] F. Primdahl, "The fluxgate magnetometer," *J. Phys. E, Sci. Instrum.*, vol. 12, no. 4, pp. 241–253, 1979.

[35] F. Primdahl, J. Petersen, C. Olin, and K. H. Andersen, "The short-circuited fluxgate output current," *J. Phys. E, Sci. Instrum.*, vol. 22, no. 6, p. 349, 1989.

[36] O. V. Nielsen et al., "Development, construction and analysis of the 'OErsted' fluxgate magnetometer," *Meas. Sci. Technol.*, vol. 6, no. 8, pp. 1099–1115, 1995.

[37] D. Gordon, R. Lundsten, and R. Chiarodo, "Factors affecting the sensitivity of gamma-level ring-core magnetometers," *IEEE Trans. Magn.*, vol. 1, no. 4, pp. 330–337, Dec. 1965.

[38] P. Ripka, *Magnetic Sensors and Magnetometers*. Norwood, MA, USA: Artech House, 2001, chs. 1–3.

[39] P. Ripka, "Review of fluxgate sensors," *Sens. Actuators A, Phys.*, vol. 33, no. 3, pp. 129–141, 1992.

[40] A. Nikitin, N. Stocks, and A. R. Bulsara, "Bistable sensors based on broken symmetry phenomena: The residence time difference vs. the second harmonic method," *Eur. Phys. J. Special Top.*, vol. 222, no. 10, pp. 2583–2593, 2013.

[41] D. Gordon, R. Lundsten, R. Chiarodo, and H. Helms, "A fluxgate sensor of high stability for low field magnetometry," *IEEE Trans. Magn.*, vol. 4, no. 3, pp. 397–401, Sep. 1968.

[42] B. Andò, S. Baglio, V. Sacco, A. Bulsara, and V. In, "Noise effects in RTD-fluxgate," in *Proc. IEEE SENSORS*, 2005, p. 4.

[43] C. Trigona, V. Sinatra, B. Andò, S. Baglio, and A. R. Bulsara, "Flexible microwire residence times difference fluxgate magnetometer," *IEEE Trans. Instrum. Meas.*, vol. 66, no. 3, pp. 559–568, Mar. 2017.

[44] P. Ripka, "Race-track fluxgate sensors," *Sens. Actuators A, Phys.*, vols. 37–38, pp. 417–421, Jun.–Aug. 1993.

[45] B. Andò, S. Baglio, S. La Malfa, C. Trigona, and A. R. Bulsara, "Experimental investigations on the spatial resolution in RTD-fluxgates," in *Proc. IEEE Instrum. Meas. Technol. Conf.*, 2009, pp. 1542–1545.

[46] C. Trigona, V. Sinatra, B. Andò, S. Baglio, and A. Bulsara, "RTD-Fluxgate magnetometers for detecting iron accumulation in the brain," *IEEE Instrum. Meas. Mag.*, vol. 23, no. 1, pp. 7–13, Feb. 2020.

CLAUDIA FERRO (Graduate Student Member, IEEE) was born in Enna, Italy, in 1996. She received the B.S. degree (cum laude) and the M.S. degree (cum laude) in electronic engineering from the University of Catania, Catania, Italy, in 2018 and 2021, respectively, where she is currently pursuing the Ph.D. degree in systems, energy, computer and telecommunications engineering.

Her M.S. thesis discussed the development and characterization of innovative measurement systems for noninvasive diagnosis of neuroferritinopathies based on fluxgate magnetometers. Her research interests include fluxgate magnetometers, microsystems, and microsensors.

BRUNO ANDÒ (Senior Member, IEEE) received the M.S. degree in electronic engineering and the Ph.D. degree in electrical engineering from the University of Catania, Catania, Italy, in 1994 and 1999, respectively.

He is currently an Associate Professor of Measurement Science with the Electric, Electronic, and Information Engineering Department, University of Catania. From 1999 to 2001, he worked as a Researcher with the Electrical and Electronic Measurement Group, University of Catania-DEES. In 2002, he became an Assistant Professor with the same staff. During his activity, he has coauthored several scientific papers, presented in international conferences and published in international journals and books. His main research interests are sensors design and optimization, inkjet printed sensors, new materials for sensors, smart multisensor architectures for environmental monitoring and AAL, and nonlinear techniques for signal processing.

Dr. Andò is currently an Associate Editor of the IEEE TRANSACTIONS ON INSTRUMENTATION AND MEASUREMENTS and the Editor-in-Chief of the *IEEE Instrumentation and Measurements Magazine*.

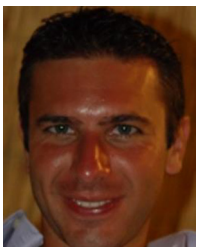

CARLO TRIGONA (Member, IEEE) received the M.S. degree (cum laude) in automation engineering and control of complex systems and the Ph.D. degree in electronic, automation, and control of complex systems from the University of Catania, Catania, Italy, in 2006 and 2010, respectively.

He is currently the Associate Professor of Electronic Instrumentations and Measurements with the Department of Electrical Electronic and Computer Engineering (DIEEI), University of Catania. From 2006 to 2009, he was a Ph.D. Student with the University of Catania. From 2010 to 2011, he worked as a Postdoctoral Fellow and a Lecturer with the University Montpellier II—LIRMM Montpellier, France, from 2011 to 2017, as a Postdoctoral Fellow and a Lecturer with DIEEI, University of Catania, and from 2017 to 2018, he worked as a Postdoctoral Fellow with the Chemnitz University of Technology, Chemnitz, Germany. From 2018 to 2020, he worked as an Assistant Professor of Electronic Instrumentation and Measurements with DIEEI, University of Catania, where he worked as a Tenure Track Professor of Electronic Instrumentation and Measurements with the same department from 2020 to 2023. He is involved in several national and international academic and engineering projects as a Coordinator and a Partner. Regarding his research activity, he has coauthored more than 200 scientific publications, with more than 2000 total citations, which include chapters in books, papers in international journals, proceedings of international conferences, and patents. His research interests include sensors, transducers, MEMS, NEMS, fluxgate magnetometers, energy harvesting, green and biodegradable sensors, and transducers based on living organisms and living sensors.

Prof. Trigona has been receiving several awards for his research activity since 2007, including the 2020 IEEE I&M Outstanding Young Engineer Award for his outstanding contribution to the advancement of I&M concept in sensors and transducers for energy harvesting. He has been contributing in the Instrumentation and Measurement community with several activities also including an editor and a reviewer for several prestigious journals since 2006.

ADI R. BULSARA received the Ph.D. degree in physics from the University of Texas at Austin, Austin, TX, USA, in 1978.

He is currently a Senior Researcher with the Space and Naval Warfare Systems Center Pacific, U.S. Navy, San Diego, CA, USA, where he heads a group that specializes in applications of nonlinear dynamics. He has authored over 100 articles in the physics literature. His current research interests include the physics of noisy nonlinear dynamic systems, with a preference for applications.

Dr. Bulsara has recently been elected a Fellow of the American Physical Society.

SALVATORE BAGLIO (Fellow, IEEE) received the M.S. (Laurea) degree in electronic engineering and the Ph.D. degree in electrical engineering from the University of Catania, Catania, Italy, in 1900 and 1994, respectively.

He is currently a Full Professor of Electronic Instrumentation and Measurements with the University of Catania, where he teaches classes on Electronic Measurements Systems and Micro and Nano Sensors. He is also a member of the Board of Ph.D. course in Electronic and Automation Engineering with the University of Catania. He has his primary scientific interests focused on development of measurement methodologies and systems based on nonlinear dynamics, development of micro and nano sensors and transducers, exploitation of material properties toward integrated transducers and on nonlinear methodologies and integrated devices for energy harvesting. He is a Principal Investigator in several scientific research projects dealing with the development of innovative sensor systems, granted by private companies and by different national and international institutions. He has authored more than 450 scientific publications, including international journals, books, conferences, and patents. At his home University, he is serving as a Deputy Rector for scientific research and as a President of the Bio-nano Research and Innovation Tower.

Prof. Baglio has been the Editor-in-Chief of the I&M Video Tutorials and the Associate Editor-in-Chief of the IEEE TRANSACTIONS ON INSTRUMENTATION AND MEASUREMENTS. He is currently the Junior Past President of the IEEE Instrumentation and Measurement Society, a member of the I&M Society AdCom, where he has served as VP Education from 2016 to 2017, an Executive Vice President from 2018 to 2019, and a President from 2020 to 2022.

Open Access funding provided by 'Università degli Studi di Catania' within the CRUI CARE Agreement